Received: 19 January 2021 | Accepted: 7 May 2021 | Published: 7 June 2021
DOI:10.20870/oeno-one.2021.55.2.4595

European grapevine moth in the Douro region: voltinism and climatic scenarios

Samuel Reis[1,*], Joana Martins[2], Fátima Gonçalves[2], Cristina Carlos[2,3] and João A. Santos[2]

[1]CoLAB VINES&WINES-National Collaborative Laboratory for the Portuguese Wine Sector, Associação para o Desenvolvimento da Viticultura Duriense (ADVID), Edifício Centro de Excelência da Vinha e do Vinho, Régia Douro Park, 5000-033 Vila Real, Portugal
[2]Centre for the Research and Technology of Agro-Environmental and Biological Sciences, CITAB, Universidade de Trás-os-Montes e Alto Douro, UTAD, 5000-801 Vila Real, Portugal
[3]ADVID, Associação para o Desenvolvimento da Viticultura Duriense, Parque de Ciência e Tecnologia de Vila Real–Régia Douro Park, 5000-033 Vila Real, Portugal

corresponding author: samuel.reis@advid.pt

Associate editor: Denis Thiery

ABSTRACT

The European grapevine moth, *Lobesia botrana* (*Lepidoptera: Tortricidae*) is considered to be the main pest in the vineyards of the Douro Demarcated Region (DDR) due to the economic losses it can cause. Damage is caused by the larvae of this pest feeding on grape clusters, rendering them susceptible to *Botrytis cinerea* in mid-season and leading to the development of primary and secondary rot at harvest. Understanding this pest´s behaviour in the region under future climate scenarios is an increasing challenge. Hence, the present study aims to assess the potential effects of two likely climate change scenarios (Representative Concentration Pathways, RCP4.5 and RCP8.5) on *Lobesia botrana* phenology, particularly at the beginning and at the peak of the three *Lobesia botrana* flights. Our findings show that the phenological events generally occur earlier in all locations and mostly during the long-term period of 2021–2080, being 7 to 12 days in advance in the RCP4.5 scenario, and 15 to 24 days in advance in RCP8.5, when compared to current values (2000–2019) and regardless of the flight number. These results suggest that a fourth complete flight is likely in the future, and that *Lobesia botrana* will become a tetravoltine species in the region. The flight (male catches) and infestation of *Lobesia botrana* over periods with daily temperatures above its upper limit of development (> 33 °C) were also analysed during the period 2000–2019 in the targeted sites. The upward trend in the number of days with maximum temperature above 33 °C tended to be accompanied by a decrease in the total number of male catches during the second and third flights, as well as a decrease in the percentage of attacked bunches by the second and third generations. Overall, climate change is expected to influence the phenology of this pest in the DDR.

KEYWORDS

Lobesia botrana, Douro Demarcated Region, vineyard, climatic scenario, phenology, upper limit development, pest management.

Supplementary data can be downloaded through: https://oeno-one.eu/article/view/4595

INTRODUCTION

The European grapevine moth, *Lobesia botrana* (Denis and Schiffermüller, 1775) (Lepidoptera: Tortricidae) - henceforth referred to as LB - is one of the most noxious vineyard pests in Europe and the Mediterranean basin (Delbac *et al.*, 2010; Ioriatti *et al.*, 2011; Caffarra *et al.*, 2012). In South America, it was spotted for the first time in Chile in April 2008 (Gilligan *et al.*, 2011). After that, sightings were also reported in California in 2009 and Argentina in 2010 (Cooper *et al.*, 2014). Lobesia larvae damage grapes by feeding on flowers and berries. However, the greatest economic losses are due to secondary infection provoked by *Botrytis cinerea* in the feeding sites of LB (Gilligan *et al.*, 2011). LB has a facultative diapause and a variable number of generations per year which depends on two main driving factors: temperature and photoperiod. In general, this moth is trivoltine in Mediterranean latitudes. Nonetheless, a fourth partial flight has been observed during the warmest years, namely in Iberian Peninsula conditions (Martín-Vertedor *et al.*, 2010; Carlos *et al.*, 2018). Voltinism is determined by a conjunction of factors: latitudinal and altitudinal gradients, which largely reflect the thermal forcing conditions of each site (Martín-Vertedor *et al.*, 2010).

In order for a pest control method (e.g., mating disruption, biocontrol agents or chemical treatments) to be efficient, it would need to be applied to pest populations during their most susceptible stages (Amo-Salas *et al.*, 2011). Pheromone traps can be used to monitor the activity of male moths in vineyards, but they require periodic visits to the field for visual observation and to record the number of catches (Ünlü *et al.*, 2019). All this field information, combined with temperature accumulation methods, is critical for implementing accurate phenological models (Riedl *et al.*, 1976; Amo-Salas *et al.*, 2011). Several models have already been developed to predict LB phenology. Some of them are based on the strong relationship between temperature accumulation (degree day (DD)) and pheromone trap catches of adult males (Milonas *et al.*, 2001; Ortega-Lopez *et al.*, 2014; Carlos *et al.*, 2018). Other authors have incorporated additional atmospheric variables (abiotic factors) in their models, such as precipitation, relative humidity or wind speed, as well as biotic factors, namely fecundity and mortality among others (Gutierrez *et al.*, 2012; Gilioli *et al.*, 2016; Castex *et al.*, 2020). From a practical point of view, such as when planning to implement decision support systems for viticulturists, DD models have several noteworthy advantages, but an important one is their relatively low complexity which facilitate their application once duly validated in terms of local conditions (Carlos *et al.*, 2018). This advantage is particularly important in regions with scarce or irregular observational data, particularly regarding the development stages of LB.

According to a recent report from the Intergovernmental Panel on Climate Change (IPCC, 2018), temperatures are likely to increase by approximately 1.5 °C between 2030 and 2052. Within this climatic context, and as already described by Thiéry *et al.* (2018), LB could indeed benefit from global warming, since the environmental temperature will be closer to its thermal optimum in many wine regions worldwide. Global warming can also indirectly affect its performance by influencing two associated trophic levels: grapevines and natural enemies, such as parasitoids (Reineke and Thiéry, 2016). Furthermore, air temperature is a key environmental factor that triggers the end of the diapause. Milder early springs are expected to promote a significant advancement in the first emergence of adults from hibernating pupae, thus impacting the voltinism of LB (Martín-Vertedor *et al.*, 2010; Reineke and Thiéry, 2016). Lastly, a combination of phenological models of grapevine (*Vitis vinifera* L.) and LB have demonstrated that an increase in temperature can result in an increase in asynchrony between the larvae resistance of grapevine growth stages and the larvae of the first generation LB (Reineke and Thiéry, 2016). Iltis *et al.* (2020) have also demonstrated that global warming could adversely impact the reproductive success of LB and the local abundance of this pest.

The Douro Demarcated Region (DDR) is located in northeastern Portugal. Since 2001 the most well-preserved part of this region, the Alto Douro Vinhateiro (ADV), has been a classified UNESCO world heritage site due to its cultural, evolutionary and living landscape (Andresen *et al.*, 2004). It is a world-renowned wine region of high natural value and exceptional biodiversity. Hence, it is of paramount importance to preserve and enhance this heritage. In the DDR, LB usually produces three generations in one year, which can cause damage to grapevine inflorescences and bunches (Carlos *et al.*, 2007). However, in warmer years, a fourth flight has been detected in early September (Carlos *et al.*, 2018), resulting in a fourth generation of damaging larvae during

TABLE 1. Geographical locations of the plots and weather stations. The corresponding sub-regions (Baixo Corgo, BC, and Cima Corgo, CC) are also indicated.

	Sub-region	Latitude (N)	Longitude (W)
Plot A	BC	41°08'48.7"	7°43'39.3"
Plot B	CC	41°9'11.70"	7°37'23.67"
Plot C	BC	41°9'15.95"	7°45'19.53"
Plot D	BC	41°9'55.86"	7°46'9.56"
WS A	BC	41°08'48.7"	7°43'39.3"
WS B	CC	41°9'19.70"	7°37' 0.90"
WS C/D	BC	41°9'12.30"	7°47' 50.60"

harvest. In terms of the impacts of climate change in the DDR, strong warming and drying trends are projected for the upcoming decades, implying overall shifts in viticultural suitability (Santos *et al.*, 2020), as well as early grapevine phenological events (Costa *et al.*, 2019; Reis *et al.*, 2020).

The aim of the present study was to assess climate change impacts on the flight phenology of LB in the DDR, thus providing valuable information to the winegrower for optimising pest control measures within an integrated pest management approach. The study was structured as follows: (1) the use of phenological models to predict LB flights under future climate change scenarios (RCP4.5 and RCP8.5) for the selected study sites and to assess any changes at the beginning of and at peak dates of the three flights, and (2) the analysis of the potential effects of temperatures above an upper limit for development (> 33 °C) on the total number of male catches (second and third flights), as well as on the percentage of bunches attacked (second and third generations), based on the analysis of historical data (2000–2019).

MATERIAL AND METHODS

1. Study area

The climate conditions in the DDR are typical of Mediterranean climates, with characteristically warm dry summers, followed by mild and rainy autumns and winters. Precipitation decreases from the west to the east of the region, with annual precipitation varying from > 1000 mm in the westernmost areas to < 400 mm in the innermost part close to the Spanish border (Fraga *et al.*, 2017). Additionally, DDR is characterised by a high interannual variability in temperature, potential evapotranspiration, total radiation and precipitation (Jones, 2013), and a large diversity of terroirs (Fraga *et al.*, 2018).

The study was carried out on four plots (A, B, C and D) located in two sub-regions of the DDR: Baixo Corgo (BC) and Cima Corgo (CC). Meteorological data from three weather stations (WS: A, B and C/D) near the four plots (< 10 km) for the period 2000–2019 were used. Figure 1 shows the geographical location of the DDR and its sub-regions, along with the locations of the aforementioned plots and WS. The geographical coordinates of all plots and WS are listed in Table 1.

2. Data collection

2.1. Pest infestation and flight

The percentage of attacked bunches (infestation) and the number of LB males caught in fixed pheromone traps were recorded during the period 2000–2019. The infestation was assessed by randomly inspecting samples of 50 to 100 inflorescences or grapes, depending on the season, during each generation of the insect. For reasons explained later, only the infestation of the second and third generations from Plot B were considered for further analysis.

2.2. LB flight models

Degree-day (DD) models to predict main LB flights were developed using data of male catches in sex pheromone traps and temperature recorded over a 20-year period, as described by Carlos *et al.* (2018). The main LB flights in the DDR were described in terms of DD required for the occurrence of its main events (beginning and peak, i.e. occurrence of 50 % of male catches).

3. Climate dataset for future scenarios

The Coordinated Regional Downscaling Experiment (CORDEX) aimed to provide an internationally coordinated framework for improving regional climate scenarios (Jacob *et al.*, 2014). The EURO-CORDEX branch

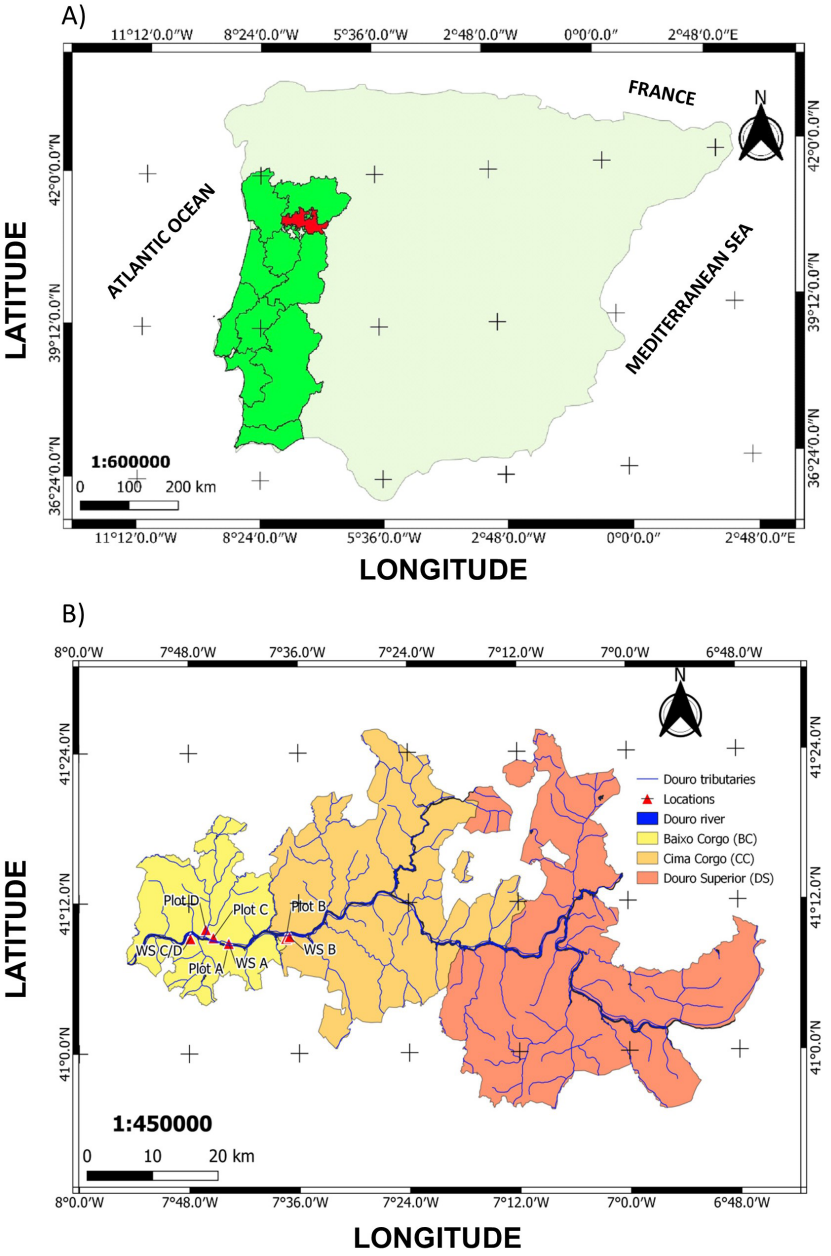

FIGURE 1. A) Map of the Iberian Peninsula showing the boundaries of the Portuguese Wine Region. The DDR is highlighted in red shading. B) Map of the DDR and locations of the plots (A, B, C and D) and weather stations (WS: A, B and C/D). The three sub-regions of DDR: Baixo Corgo (BC, yellow), Cima Corgo (CC, orange) and Douro Superior (DS, red) are also depicted, along with the main watercourses (the Douro/Duero River) represented by a thick blue line.

generated European-wide climate simulations under different future scenarios. A large set of simulations is currently available as a result of dynamic downscaling experiments which ran Global Climate Model (GCM)–Regional Climate Model (RCM) chains (Spinoni *et al.*, 2020). The climate model simulations selected for the present study are listed in Table 2. Gridded T_X (maximum temperature) and T_N (minimum temperature) for a historical period (1981–2015) and a future period (2021–2080) in RCP4.5 and RCP8.5 were used to carry out analyses for the short-term (2021–2040), medium-term (2041–2060) and long-term (2061–2080) periods. The simulated data were available at an 11 km grid resolution and were trimmed for a sector covering the DDR.

As climate simulations may be affected by significant biases with respect to real-world climate, the E-OBS observational dataset was used

TABLE 2. Combinations of Global Climate Model (GCM) and Regional Climate Model (RCM) runs available for Europe and their references.

GCM	References	RCM	References	Abbreviation
CNRM-CM5	(Voldoire *et al.*, 2013)	CNRM-ALADIN53	(Lucas-Picher *et al.*, 2013; Tramblay *et al.*, 2013)	CNRMALADIN
ICHEC-EC-EARTH	(Hazeleger *et al.*, 2010; Koenigk *et al.*, 2013)	DMI-HIRHAM5	(Christensen *et al.*, 2007)	ICHECDMI
IPSL-CM5A-MR	(Dufresne *et al.*, 2013)	IPSL-INERIS-WRF331F	(Menut *et al.*, 2013)	IPSLINERIS
MPI-ESM-LR	(Giorgetta *et al.*, 2013)	CLMcom-CCLM4.8-17	(Rockel *et al.*, 2008)	MPICLM

to calibrate the model data within the DDR sector. The E-OBS dataset (available at https://www.ecad.eu/download/ensembles/download.php) is a European high resolution and daily gridded observational dataset for average minimum and maximum temperatures and total precipitation (Cornes *et al.*, 2018). The data were developed as part of the ENSEMBLES project (European Union Framework 6) to be used in climate change studies and for the validation of regional climate models (Haylock *et al.*, 2008; Hofstra *et al.*, 2009; Kyselý and Plavcová, 2010). To correct model biases, a quantile mapping approach (Amengual *et al.*, 2011; Miao *et al.*, 2016) was applied to the simulated data using E-OBS as a baseline and the common historical period of 1981–2015 as a reference. In this context, the bias-corrected gridded temperatures (T_N and T_X) were extracted from the grid points which were closest to the selected plots. The extracted grid points were E-OBS A and B (41°11'15"N and 7°41'15"W) and E-OBS C/D (41°11'15"N and 7°48'45"W).

Subsequently, linear regression adjustments between WS and E-OBS data were carried out (two linear regressions for each WS, T_N and T_X; i.e., six transfer functions in total). The corresponding linear regression equation (transfer function) was then applied to climate model data to adjust the bias-corrected simulations of local climatic conditions. It was assumed that the transfer functions already identified in the historical period between E-OBS and WS would remain mostly unchanged for the future period. This late adjustment was a critical point in the analysis, as the results of the phenology models are very sensitive to the actual temperature observed on a specific site.

4. Trend analysis and statistical significance

Although linear regression equations are frequently adjusted to time series for the initial detection and estimation of trends (which is a reasonable approach when the coefficient of determination (R-squared) associated with the linear trend is relatively high), climate change trends are frequently non-linear throughout the study period. Hence, the assessment of the statistical significance of trends in a time series should be also carried out using non-parametric hypothesis tests. The Mann-Kendall (MK) is a non-parametric test used to statistically assess whether there is either an upward or downward trend in the parameters of interest (Mann, 1945; Kendall, 1975). The significance of the MK test can be verified with a bilateral test (1) by applying the standardized Z statistics described by Yenigun *et al.* (2008):

$$Z = \begin{cases} \frac{S-1}{\sqrt{var(S)}} & S > 0 \\ 0 & S = 0 \\ \frac{S+1}{\sqrt{var(S)}} & S < 0 \end{cases} \quad (1)$$

which is used to test the null hypothesis (H_0).

The positive value of Z indicates an upward trend ($|Z| > 0$), while a negative value indicates a downward trend ($|Z| < 0$). To test the increasing or decreasing trend in the significance level α, the H_0 is rejected if the absolute value of Z is greater than $Z_{\alpha/2}$ ($|Z| > Z_{\alpha/2}$) (Moreira and Naghettini, 2016). In this study, the MK test was used at a significance level of 0.1 %, $p \leq 0.001$ (i.e., confidence level of 99.9 %) for testing monotonic trends at the beginning and peak dates (in DOY) of LB flights (three flights) under RCP4.5 and RCP8.5.

The MK test can be used to detect statistically significant trends, but it does not provide their magnitude. Therefore, the MK test was complemented by Sen's slope estimator, initially proposed by Sen (1968) and described according to Hirsch *et al.* (1982) by (2):

$$D_{iy} = \left[\frac{Y_j - Y_i}{X_j - X_i}\right] \quad 1 \le X_i < X_j \le N \qquad (2)$$

where and represent the years within the period 2021–2080 in the *i*-th and *j*-th time instant respectively and for both scenarios (RCP4.5 and RCP8.5). Lastly, the magnitude of the trend is estimated by the median of two values of D_{iy}.

5. Effects of warmer conditions on pest infestation and flight

The potential effects of high temperatures on the number of LB male catches and infestation were also examined. A preliminary analysis was carried out on plot B, as it provided a larger sample of observed data for the percentage of attacked bunches and the total number of male catches. The aforementioned data was related to the number of days with maximum temperature, T_X, above 33 °C during the second generation/flight (2000–2019: fifteen years with % of attacked bunches/thirteen years of the total number of catches) and third-generation/flight (2000–2019: eleven years with % of attacked bunches/thirteen years of the total number of catches). The number of days with maximum temperature above 33 °C is counted in the relevant months; i.e., when the second (June-July) and third (July-September) flights/generations took place. Lastly, the infestation and male LB catches at high temperatures (> 33 °C; i.e., above the upper limit) were also analysed to gain an understanding of the impact of excessively high temperatures on an LB population (Briere and Pracros, 1998).

To predict the impact of future climate scenarios on LB flights, the three non-linear models described by Carlos *et al.* (2018) for predicting each LB flight were used, with 1 January as the starting point for DD accumulation. Therefore, the models and the corrected T_N and T_X from 2021-2080 (corresponding WS and plots) for both RCP4.5 and RCP8.5 were automatically run in computational code. The output comprised the simulated days (in Julian days of the year (DOY)) of the beginning and peak (corresponding to 50 % of male catches) of each LB flight.

RESULTS

1. Correction of model climate data with observations

In order to assess the consistency between E-OBS and local WS data, T_N and T_X recorded at the different WS (A, B and C/D) and obtained from the E-OBS dataset (A, B and C/D) were correlated. The Pearson product-moment correlation coefficients and the corresponding determination coefficients were estimated. This correlation analysis was also complemented by fitting linear regression lines to the corresponding scatterplot diagrams. For this purpose, E-OBS A and B data were correlated with observed data from WS A and B (at the same location as plots A and B respectively), whereas E-OBS C/D data were correlated with WS C/D (the same location as C and D plots). Hence, a total of six linear regressions (three for T_N and three for T_X) were carried out and their respective parameters were estimated following a least-squares approach.

Overall, statistically significant correlation coefficients at a 99 % confidence level were obtained. Moreover, the correlation coefficients were higher than 0.94 for all regressions, comfirming very robust correlations between both datasets. Accordingly, very high determination coefficients (percentage of variance explained by the linear regression model) were obtained, ranging from 89 % to 98 % (Figure 2 A, B, C, D, E and F).

Although the data pairs tend to be well-aligned in clouds close to the corresponding regression lines, some discrepancies are worth mentioning. This is particularly true for T_X in WS B, where several days with maximum temperatures close to 0 ºC were observed in the WS and much higher values were obtained from E-OBS. In terms of T_N there were also a few days with similar discrepancies. These discrepancies weaken the linear association between the WS and E-OBS time series. After a more thorough analysis of these specific days, it was found that almost all of them occurred during the winter period (December to February) when strong thermal inversions occurred in the region; these thermal inversions were associated with settled weather conditions driven by strong and nearly-stationary anticyclonic systems located over the Iberian Peninsula (not shown). Such conditions contribute to the formation of thick fog layers in the deep valleys of the region, which can sometimes persist for several days when solar radiation levels are not high enough to dissipate the fog during the day, which is subsequently reinforced at night by mountain breezes and katabatic winds that drain cool air masses to the low-elevation areas of the Douro River basin. The other WS were less prone to these events. In addition, the development and the end of the diapause (Tobin *et al.*, 2001; Tobin *et al.*, 2002)

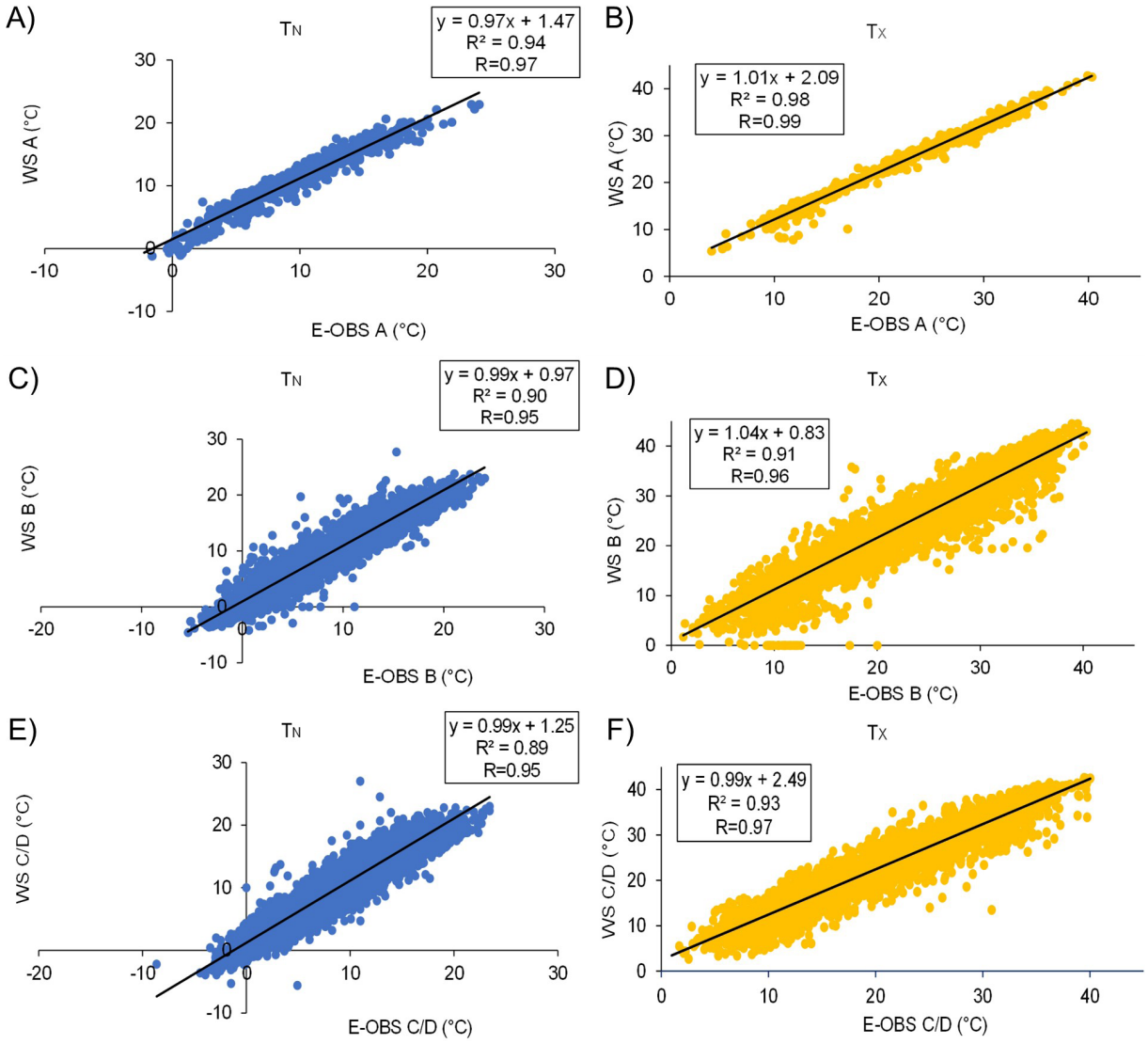

FIGURE 2. Scatterplot diagrams between E-OBS (A, B and C/D) and observed temperatures (T_N and T_X in ºC; blue and yellow dots respectively) from weather stations (WS: A, B and C/D) near the plots (A, B and C/D respectively). The corresponding linear regression lines are also shown, as well as the respective regression equations, the determination coefficient (R-squared) and the correlation coefficient (R).

of the majority of multivoltine insects described by Tobin *et al.* (2008) are driven by temperature, while the beginning of the diapause is driven by photoperiod (Nagarkatti *et al.*, 2001). Under regional conditions, the projected increase in temperature could bring forward the end of the diapause of individuals emerging in spring, with an earlier first flight of LB.

Owing to the aforementioned noteworthy consistency between E-OBS and WS data, these linear regressions were then used to calibrate the climate model data to site conditions over the future period and for both scenarios (RCP4.5 and RCP8.5). This is a common procedure for correcting bias in the mean (location) and variance (scale), which guarantees that local weather conditions will be more accurately represented in both E-OBS and climate model data. Other more advanced methodologies, like quantile mapping approaches, are not recommendable when only short temporal periods are available (small sample sizes), as is the case of the WS time series being analysed here. The intercepts of the linear regression equations show some important biases in the mean, varying from nearly 0.8 to 2.5 ºC (all of them positive), which implies that the WS temperatures are systematically higher than in E-OBS and significant corrections in the

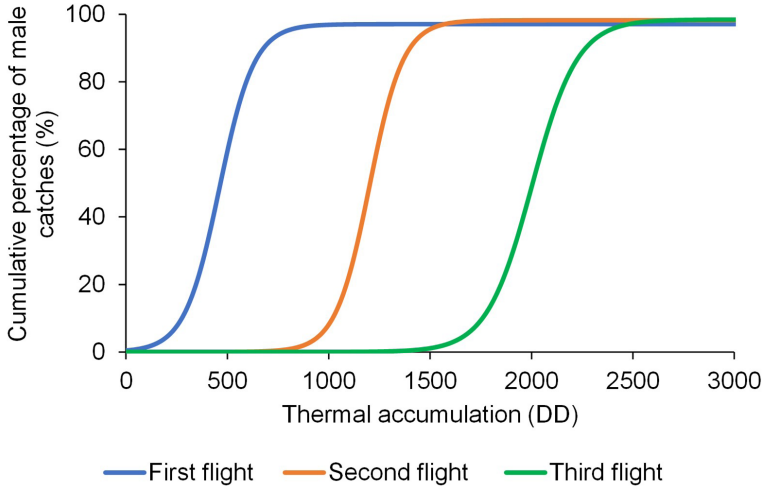

FIGURE 3. Cumulative percentage of male catches of LB for the first, second and third flights in relation to accumulated DD, with 1 January as a starting point for DD accumulation.

means were applied to E-OBS data. The slopes of the linear regression equations vary from approximately 0.97 to 1.04, which means that the variance is similar in both datasets, and only slight corrections were applied to the E-OBS variances.

2. Climatic projections and impacts on LB

2.1. LB flight

The bias-corrected and site-adjusted daily mean temperatures for the future climatic scenarios (RCP4.5 and RCP8.5) were used as input for the three previously defined models of each flight (Figure 3). The simulated days of the beginning and peak dates of LB male flights for each GCM-RCM model chain (CNRMALADIN, ICHECDMI, IPSLINERIS and MPICLM) were then obtained.

2.2. Simulations for future scenarios

The simulated days for the beginning and peak dates of the LB flights were obtained for each combination of location (four), flight (three), climate scenario (two) and climate model (four) separately. Figures 4 and S1 (Supplementary Material) show the box-plot diagrams for RCP4.5 and RCP8.5 respectively, in which all the models and years within a given period are pooled. Although there is a significant spread within each sub-period (short, medium and long-term) and flight (roughly 35–60 days), there is a clear and consistent trend in earlier beginning and peak dates of the different LB flights and for all plots.

For the sake of succinctness, the equally weighted ensemble averages for the four climate models were calculated, keeping the other parameters separate (scenario, location and flight number). The ensemble averages were thoroughly analysed in this study, as they are central tendency measures which can be used as an indicator for climate model experiments, which are all considered equally valid. Figures S2 and S3 show the chronograms of the interannual variability of the ensemble averages of the LB beginning and peak flight dates (DOY) during the period 2021–2080 for each location and flight curve and in the RCP4.5 and RCP8.5 scenarios respectively.

For all flights and locations (Figures S2 and S3), there is a general shift to earlier beginning and peak flight dates (downward trends) when compared to the present conditions (2000–2019). Not surprisingly, the trends are generally more significant in RCP8.5 than in RCP4.5, as the former scenario is related to a much stronger radiative anthropogenic forcing, with more accentuated upward trends in temperature. To complement the information in the chronograms, the values of the linear regression trends of the ensemble averages are shown in Table 3.

For the first LB flight and all locations (Figures S2 and S3, Table 3), the flight beginning and peak dates in both scenarios (RCP4.5 and RCP8.5) were somewhat in advance. Over one decade, the earliness in both beginning and peak dates varies from 1 to 2 days with respect to the present values in RCP4.5 and up to 3 days in the severest scenario (RCP8.5). For the whole period (60 years), the trend in early beginning of flight is evident for all locations in the RCP4.5 scenario: in plot B it was 8 days early and in plots A and C/D it was 7 days earlier. The flight peak in the same scenario and for all locations was projected as being 10 days

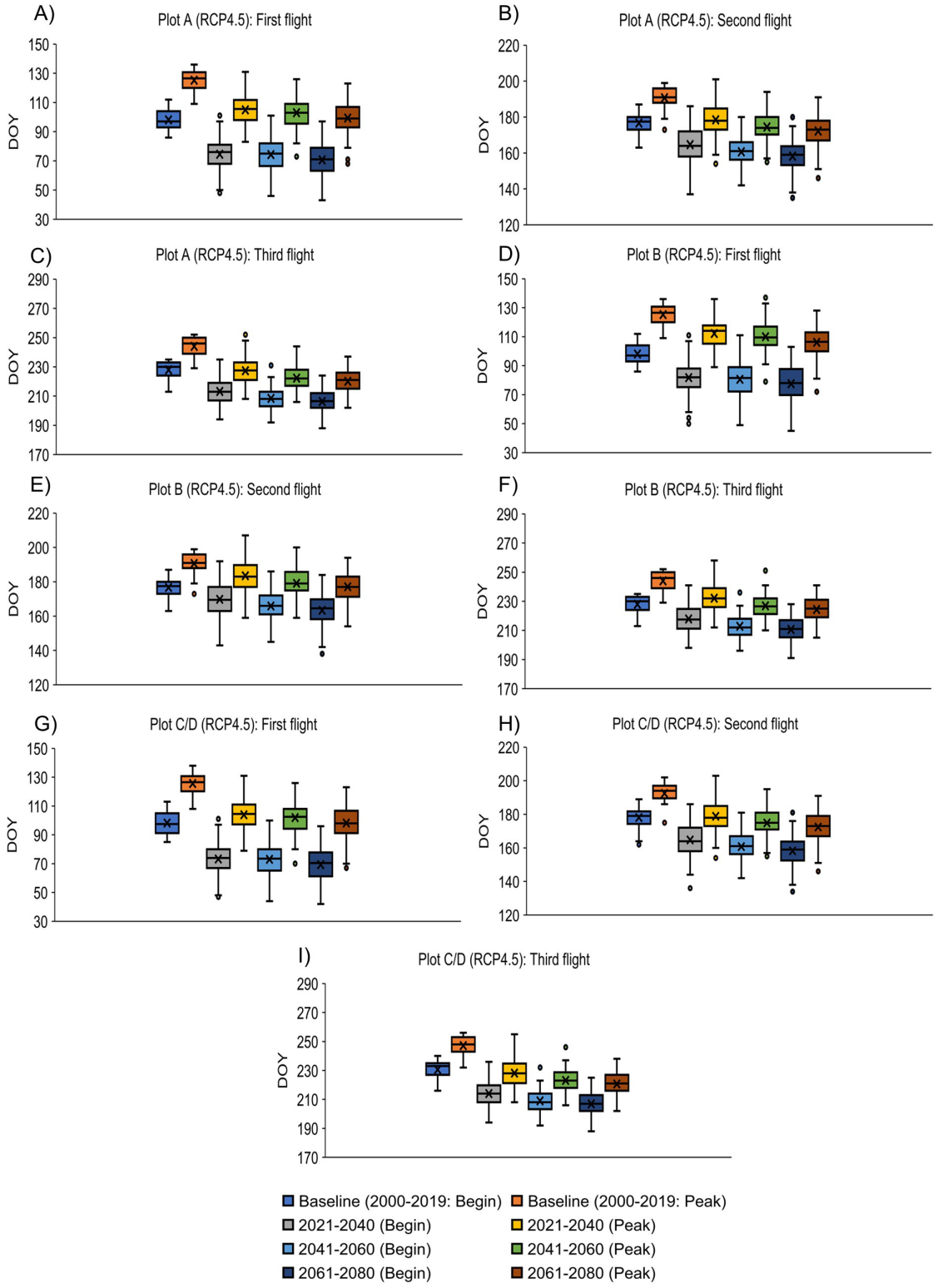

FIGURE 4. Box-plot diagrams of the beginning and peak dates (DOY) of the LB first, second and third flights for the outlined plots (A, B, C and D) over baseline (2000-2019), short-term (2021–2040), medium-term (2041–2060) and long-term (2061–2080) periods in climate scenario RCP4.5. See legend for details. The × represents the average, and the solid line within the boxes the median. The box upper (lower) limit corresponds to the third (first) quartile, while the whiskers correspond to the non-outlier extremes. Outliers (black circles) are considered as values above/below the box upper/lower limit by a factor of 1.5 × IQR (Interquartile Range; i.e., box height).

TABLE 3. LB flight events (days) for the beginning and peak (three flights) with respect to baseline (2000–2019) in RCP4.5 and RCP8.5 scenarios, as a function of the vineyard plots (A, B and C/D). The linear trends: per year, decade and 60-year period.

Flight	Period	Plot	Begin* (RCP4.5)	Peak* (RCP 4.5)	Begin* (RCP8.5)	Peak* (RCP8.5)
First	Annual	A	–0.1	–0.2	–0.3	
		B				
		C/D				
	Decadal	A	–1.0	–2.0	–3.0	
		B				
		C/D				
	60 years	A	–7.0	–10.0	–15.0	–18.0
		B	–8.0		–17.0	–20.0
		C/D	–7.0		–15.0	–18.0
Second	Annual	A	–0.2		–0.4	
		B				
		C/D				
	Decadal	A	–2.0		–4.0	
		B				
		C/D				
	60 years	A	–10.0		–22.0	–21.0
		B			–22.0	
		C/D			–22.0	
Third	Annual	A	–0.2		–0.4	
		B				
		C/D				
	Decadal	A	–2.0		–4.0	
		B				
		C/D				
	60 years	A	–11.0	–12.0	–22.0	–23.0
		B	–12.0		–23.0	–24.0
		C/D	–11.0		–23.0	–23.0

*Days in advance with respect to the present.

in advance. However, in the RCP8.5 scenario, flights began 15 and 17 days in advance in plots A/C/D and plot B respectively, while the flight peak was 20 days in advance in plot B and 18 days in advance in the other plots. In general, at the end of the evaluated period and regardless of location, flights were in advance by 7 to 10 days in RCP4.5 and 15 to 20 days in RCP8.5.

Over a period of sixty years, the beginning and peak dates of the second LB flight (Figures S2 and S3; Table 3) in all locations were 10 and 22 days in advance in RCP4.5 and RCP8.5 respectively, except for plot A in RCP8.5 for which the peak of

TABLE 4. Sen´s slope estimator applied to the DOY series for the beginning and peak of LB flights in plot A in the different scenarios (RCP4.5 and RCP8.5) and over the period 2021–2080. According to the Mann-Kendall test, all slopes are statistically significant at a confidence level of 99.9 % ($p \leq 0.001$).

Plot		Sen´s slope estimator*	
		RCP4.5	RCP8.5
A	First flight (Beginning)	–1.11*e*-01	–2.50*e*-01
	First flight (Peak)	–1.67*e*-01	–2.99*e*-01
	Second flight (Beginning)	–1.67*e*-01	–3.67*e*-01
	Second flight (Peak)	–1.60*e*-01	–3.55*e*-01
	Third flight (Beginning)	–1.78*e*-01	–3.59*e*-01
	Third flight (Peak)	–1.88*e*-01	–3.75*e*-01

*Mann-Kendall test at the significance level of 0.1 % ($p \leq 0.001$)

flight was 21 days earlier. It is therefore important to highlight the general ealier dates in all locations and for all flight periods, ranging from –10 days in RCP4.5 and –21 to –22 days in RCP8.5 from the period under evaluation to the present.

At the end of the period of the third LB flight (Figures S2 and S3; Table 3) the beginning of the flights were 11 days earlier for plots A and C/D and 12 days earlier for plot B. The peak flight date was 12 days in advance in all locations. A clear trend can be observed for the most severe climate scenario: beginning of flight in Plot B was 23 days earlier and the flight peak was 24 days earlier. In general, at the end of the period, the beginning and peak of flights were 11–12 days in advance in RCP4.5 and 22–24 days in the most severe climate scenario.

Therefore, these results show that in both climatic scenarios pest phenological events are projected to occur earlier and voltinism to strengthen in the future.

To better document the inter-model variability, the minimum and maximum DOY for each variable have also been depicted (Figures S2 and S3). Although the spread among models is apparent, there is no evidence for a change in the model uncertainty throughout the future period.

An assessment was carried out on the statistical significance of the identified trends in LB flight beginning and peak dates for the full period of 2021–2080 in all locations and climatic scenarios (RCP4.5 and RCP8.5). The application of the MK trend test on plot A (Table 4) shows *p*-values below the 0.1 % ($p \leq 0.001$) significance level, regardless of flight and climatic scenario; H_0 can thus be rejected, verifying a significant trend in the analysed series. The Sen´s slope estimator generally varied between –1.11*e*-01 and –3.75*e*-01. Similar results were found for the remaining plots (not shown). Therefore, these values confirm the statistical significance of the identified downward trends in both the beginning and peak dates of the LB flights.

3. Effects of extreme temperatures versus pest infestation and male catches

The likely implications of very warm weather conditions on the LB population are only briefly evaluated here, as the sample size of observed data is very limited. An illustrative analysis was carried out on plot B for percentage of attacked bunches and the total number of adult male catches based on the evolution of these parameters over the period 2000–2019. The results are shown in Figure 5.

For the second generation, an increase in the number of days above 33 °C (June-July) and a decrease of 1.7 % in bunches attacked per year was observed. Moreover, less than 17 male catches were observed in the delta traps on the second flight. For the third generation, the same trend as the second one was observed, with the number of days above 33 °C (July-September) also increasing and the attacked bunches decreasing by 0.8 %, and with 10 catches on the third flight.

DISCUSSION

The results obtained in this study show a considerable warming trend in the studied locations of the DDR in the upcoming decades. The temperature increase projected for the climate scenarios (RCP4.5 and RCP8.5) is in line with

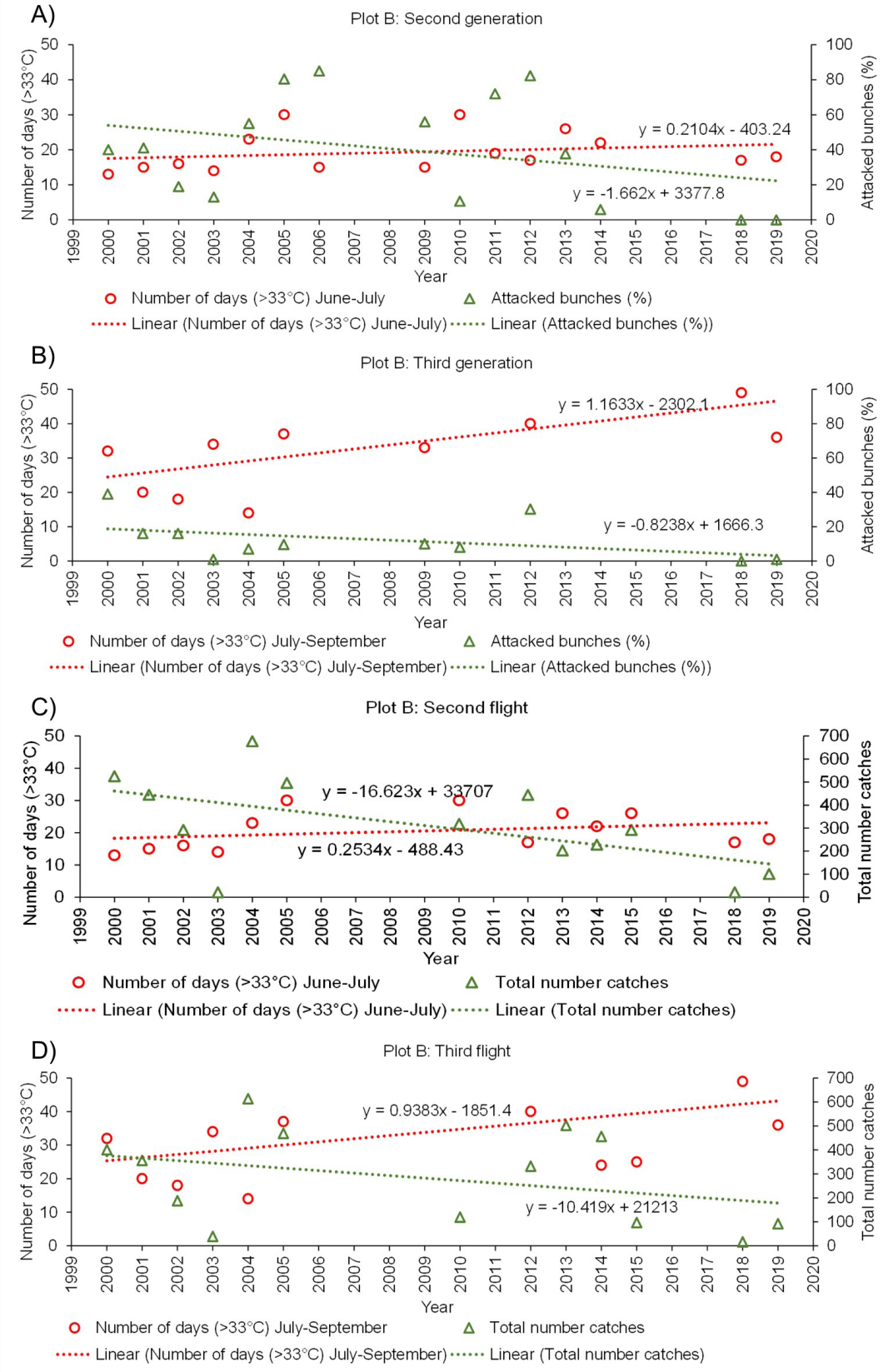

FIGURE 5. Chronograms of the number of days with maximum temperature above 33 °C during the outlined relevant periods versus % of attacked bunches (A and B panels for the second and third generations respectively) and the total number of male catches (C and D panels for the second and third flights respectively) in plot B over the period 2000–2019.

those already reported (IPCC, 2018); i.e., an increase of 1.5 °C in the period 2030–2052. In the analysis of the phenological activity of LB, models of three flights previously validated with data exclusively from DDR were applied to the regional future projections.

Our results indicate generally earlier LB flight dates throughout the period 2021–2080 in the two different climatic scenarios RCP4.5 and RCP8.5 compared to the present (2000–2019). Overall, the LB flights in all locations at the end of the period were 7 to 12 days in advance in RCP4.5, and 15 to 24 days in advance in RCP8.5, regardless of the flight. The earliness of the LB flights in these climatic scenarios is in line with other similar studies (Martín-Vertedor *et al.*, 2010; Caffarra *et al.*, 2012; Reineke and Thiéry, 2016; Taylor *et al.*, 2018). Changes in phenology due to global warming have been demonstrated for pests other than this lepidopteran (Gutierrez *et al.*, 2008; Andrew and Hill, 2017). The significant earliness of the three LB flights in both climatic scenarios (RCP4.5 and RCP8.5) and the period 2021-2080 suggests that a complete fourth flight could happen in the future in the DDR as occured in Spain in 2006 (Martín-Vertedor *et al.,* 2010). Forister and Shapiro (2003) analysed adults of 23 species of Lepidoptera in the Central Valley of California and found that the first flight date had advanced over the past 31 years. Furthermore, Stefanescu *et al.* (2003) analysed data from a trap in the period 1988–2002 in Spain and reported that the average date of the first flight of 8 species was significantly advanced. In a study conducted in southwest Australia, the flight of *Heteronympha merope was* found to occur on average 1.5 days earlier per decade over 65 years (1941-2005), owing to an average temperature increase in this period of 0.16 °C per decade (Kearney *et al.*, 2010). The effects of climate change on these species (Lepidoptera) have thus had a visible impact on their phenology (Hufnagel and Kocsis, 2011), which is confirmed by the results observed in this study.

Until the end of this century, the increase in voltinism will be more likely due to warming, since at higher temperatures faster development could lead to additional generations of multivoltine species, as is the case with the grape moth, and as supported by previous studies (Altermatt, 2010; Reineke and Thiéry, 2016). In addition, the increase in temperature may advance the end of the diapause of individuals emerging in spring, with an earlier first flight. On the other hand, over the past few years, due to climate change, the phenological events of grapevine are occuring earlier, specifically budburst, flowering, veraison and ripening. According to Costa *et al.* (2019), in the DDR, the budburst, flowering and veraison of cv. *Touriga Nacional* and *Touriga Franca* are projected to occur 6-8 and 10-12 days earlier respectively until the end of the century. Jones (2007) has found a strong relationship between phenological timings and observed warming, with phenological events occuring 6 to 25 days early in various grapevine varieties and locations. Other studies have revealed similar findings (Ramos, 2017; Reis *et al.*, 2020). Both LB and *Vitis vinifera* L. can therefore be expected to undergo significant shifts in their phenology with increasing temperatures, though their interaction is not yet fully understood and requires further research in forthcoming studies.

The results obtained in the present study indicate that there is a relationship between the number of days with maximum temperature above 33°C and the population dynamics observed in the second and third generations/flights, in particular in the precentage of attacked bunches/total number of male captures. According to Woiwod (1997), besides influencing phenology, climate change can also lead to changes in species abundance. Gutierrez *et al.* (2012) found that LB abundance levels decreased in hot deserts in southern California, where temperatures frequently surpass their upper thermal limit. Another study by Gutierrez *et al.* (2018) reported that LB levels decreased in dry and warm areas, such as southwestern Spain or Morocco, where high summer temperatures which were near or exceeded the upper limit adversely affected their vital rate. Iltis (2019) suggests that heatwaves can have important implications for the defensive abilities of LB against its natural enemies, predisposing natural populations to attack by larval parasitoids. Moreover, a recent study by the same author (Iltis *et al.*, 2020) suggests that climate change could reduce the abundance of this pest over generations in Eastern France, due to the negative effects of the local warming scenario observed for adult LB lifespan and its reproductive success. Further research should be carried out in the DDR to better assess the effects of excessively high temperatures on LB population dynamics, as in the present study only a preliminary assessment was carried out.

The use of phenological models to predict LB development in the DDR should be improved in future research by, for example, collecting more

field data (from eggs and larval stages) to ensure the fine-tuning of model parameters and thresholds to the actual conditions, or by incorporating new abiotic and biotic factors in the model. The use of atmospheric elements, like precipitation, wind speed or relative humidity, could improve model performance and its corresponding prediction capacity, which will be of foremost relevance to viticulturists in the DDR.

CONCLUSIONS

In this study, a new methodology was implemented to evaluate the impact of future climate scenarios in the DDR on LB evolution. Future warming imples a generalised shift to earlier beginning and peak dates of the three LB flights in the studied locations. A fourth complete flight in the future is therefore increasingly likely, LB thus becoming a tetravoltine species, leading to greater voltinism. Conversely, the number of days with excessively high temperatures (i.e., above the upper threshold for development (> 33 °C)), is projected to increase in the future. This will result in a decrease in the total number of male catches in the traps (second and third flights) and the percentage of bunches attacked (second and third generations), which is already being recorded in association with above-optimal temperatures. Therefore, excessively high temperatures could have implications for LB populations and their defensive ability against natural enemies. This could be valuable information for winegrowers in the future to optimise control measures for LB within an integrated pest management approach.

Acknowledgements: This research was funded by the operation nº NORTE-06-3559-FSE-000067 and by the Clim4Vitis project "Climate change impact mitigation for European viticulture: knowledge transfer for an integrated approach", which is funded by European Union's Horizon 2020 Research and Innovation Programme, under grant agreement nº810176. The authors from CITAB were also supported by National Funds by FCT - Portuguese Foundation for Science and Technology, under the project UIDB/04033/2020. Finally, the authors would also like to thank ADVID and its members for providing meteorological data from weather stations and for collaborating in the field data collection, specifically damage assessment and counting of traps.

REFERENCES

Altermatt, F. (2010). Climatic warming increases voltinism in European butterflies and moths. *Proceedings of the Royal Society B: Biological Sciences, 277*(1685), 1281-1287.

Amengual, A., Homar Santaner, V., Romero, R., Alonso, S., & Ramis, C. (2011). Projections of the climate potential for tourism at local scales: Application to Platja de Palma, Spain. *International Journal of Climatology, 32*. doi:10.1002/joc.2420

Amo-Salas, M., Ortega-López, V., Harman, R., & Alonso-González, A. (2011). A new model for predicting the flight activity of Lobesia botrana (Lepidoptera: Tortricidae). *Crop Protection, 30*, 1586-1593. doi:10.1016/j.cropro.2011.09.003

Andresen, T., de Aguiar, F. B., & Curado, M. J. (2004). The Alto Douro Wine Region greenway. *Landscape and Urban Planning, 68*(2), 289-303. https://doi.org/10.1016/S0169-2046(03)00156-7

Andrew, N., & Hill, S. (2017). Effect of Climate Change on Insect Pest Management (pp. 195-223).

Briere, J. F., & Pracros, P. (1998). Comparison of Temperature-Dependent Growth Models with the Development of Lobesia botrana (Lepidoptera: Tortricidae). *Environmental Entomology, 27*(1), 94-101. doi:10.1093/ee/27.1.94

Caffarra, A., Rinaldi, M., Eccel, E., Rossi, V., & Pertot, I. (2012). Modelling the impact of climate change on the interaction between grapevine and its pests and pathogens: European grapevine moth and powdery mildew. *Agriculture, Ecosystems & Environment, 148*, 89-101. https://doi.org/10.1016/j.agee.2011.11.017

Carlos, C., Alves, F., & Torres, L. (2007). *Ciclo biológico da traça da uva, Lobesia botrana (Den. & Schiff.), na Região Demarcada do Douro.* Paper presented at the 7º Simpósio de Vitivinicultura do Alentejo.

Carlos, C., Gonçalves, F., Oliveira, I., & Torres, L. (2018). Is a biofix necessary for predicting the flight phenology of Lobesia botrana in Douro Demarcated Region vineyards? *Crop Protection, 110*, 57-64. doi:10.1016/j.cropro.2017.12.006

Castex, V., García de Cortázar-Atauri, I., Calanca, P., Beniston, M., & Moreau, J. (2020). Assembling and testing a generic phenological model to predict Lobesia botrana voltinism for impact studies. *Ecological Modelling, 420*, 108946. https://doi.org/10.1016/j.ecolmodel.2020.108946

Christensen, O., Drews, M., Christensen, J., Dethloff, K., Hebestadt, I., Ketelsen, K., & Rinke, A. (2007). The HIRHAM regional climate model version 5 (beta). *DMI Technical Report 06-17*.

Cooper, M. L., Varela, L. G., Smith, R. J., Whitmer, D., Simmons, G., Lucchi, A., . . . Steinhauer, R. (2014). MANAGING NEWLY ESTABLISHED PESTS: Growers, scientists and regulators collaborate on European grapevine moth program. *California Agriculture, 68*(4), 125-133. doi:10.3733/ca.v068n04p125

Cornes, R. C., van der Schrier, G., van den Besselaar, E. J. M., & Jones, P. D. (2018). An Ensemble Version of the E-OBS Temperature and Precipitation Data Sets. *Journal of Geophysical Research: Atmospheres, 123*(17), 9391-9409. https://doi.org/10.1029/2017JD028200

Costa, R., Fraga, H., Fonseca, A., García de Cortázar-Atauri, I., Val, M. C., Carlos, C., . . . Santos, J. A. (2019). Grapevine phenology of cv. touriga franca and touriga nacional in the Douro wine region: Modelling and climate change projections. *Agronomy, 9*(4), 210.

Delbac, L., Lecharpentier, P., & Thiery, D. (2010). Larval instars determination for the European Grapevine Moth (Lepidoptera: Tortricidae) based on the frequency distribution of head-capsule widths. *Crop Protection, 29*, 623-630. doi:10.1016/j.cropro.2010.01.009

Dufresne, J. L., Foujols, M. A., Denvil, S., Caubel, A., Marti, O., Aumont, O., . . . Vuichard, N. (2013). Climate change projections using the IPSL-CM5 Earth System Model: from CMIP3 to CMIP5. *Climate Dynamics, 40*(9), 2123-2165. doi:10.1007/s00382-012-1636-1

Forister, M., & Shapiro, A. (2003). Climatic trends and advancing spring flight of butterflies in lowland California. *Global Change Biology, 9*, 1130-1135. doi:10.1046/j.1365-2486.2003.00643.x

Fraga, H., Costa, R., & Santos, J. A. (2018). Modelling the Terroir of the Douro Demarcated Region, Portugal. *MATEC Web of Conferences, 50*, 02009. doi:10.1051/e3sconf/20185002009

Fraga, H., García de Cortázar Atauri, I., Malheiro, A. C., Moutinho-Pereira, J., & Santos, J. A. (2017). Viticulture in Portugal: A review of recent trends and climate change projections. *OENO One, 51*(2), 61-69. doi:10.20870/oeno-one.2017.51.2.1621

Gilioli, G., Pasquali, S., & Marchesini, E. (2016). A modelling framework for pest population dynamics and management: An application to the grape berry moth. *Ecological Modelling, 320*, 348-357. doi:10.1016/j.ecolmodel.2015.10.018

Gilligan, T., Epstein, M., Passoa, S., Powell, J., Sage, O., & Brown, J. (2011). Discovery of Lobesia botrana ([Denis & Schiffermuller]) in California: An Invasive Species New to North America (Lepidoptera: Tortricidae). *Proceedings- Entomological Society of Washington, 113*, 14-30. doi:10.4289/0013-8797.113.1.14

Giorgetta, M. A., Jungclaus, J., Reick, C. H., Legutke, S., Bader, J., Böttinger, M., . . . Stevens, B. (2013). Climate and carbon cycle changes from 1850 to 2100 in MPI-ESM simulations for the Coupled Model Intercomparison Project phase 5. *Journal of Advances in Modeling Earth Systems, 5*(3), 572-597. doi:10.1002/jame.20038

Gutierrez, A. P., Daane, K. M., Ponti, L., Walton, V. M., & Ellis, C. K. (2008). Prospective evaluation of the biological control of vine mealybug: refuge effects and climate. *Journal of Applied Ecology, 45*(2), 524-536. https://doi.org/10.1111/j.1365-2664.2007.01356.x

Gutierrez, A. P., Ponti, L., Cooper, M. L., Gilioli, G., Baumgärtner, J., & Duso, C. (2012). Prospective analysis of the invasive potential of the European grapevine moth Lobesia botrana (Den. & Schiff.) in California. *Agricultural and Forest Entomology, 14*(3), 225-238.

Gutierrez, A. P., Ponti, L., Gilioli, G., & Baumgärtner, J. (2018). Climate warming effects on grape and grapevine moth (Lobesia botrana) in the Palearctic region. *Agricultural and Forest Entomology, 20*(2), 255-271.

Haylock, M. R., Hofstra, N., Tank, A. M. G., Klok, E. J., Jones, P., & New, M. (2008). A European daily high-resolution gridded dataset of surface temperature and precipitation. *J. Geophys. Res., 113*, D20119. doi:10.1029/2008JD10201

Hazeleger, W., Severijns, C., Semmler, T., Ştefănescu, S., Yang, S., Wang, X., . . . Willén, U. (2010). EC-Earth: A Seamless Earth-System Prediction Approach in Action. *Bulletin of the American Meteorological Society, 91*(10), 1357-1364. doi:10.1175/2010bams2877.1

Hirsch, R. M., Slack, J. R., & Smith, R. A. (1982). Techniques of trend analysis for monthly water quality data. *Water Resources Research, 18*(1), 107-121. https://doi.org/10.1029/WR018i001p00107

Hofstra, N., Haylock, M. R., New, M., & Jones, P. (2009). Testing E-OBS European high-resolution gridded data set of daily precipitation and surface temperature. *Journal of Geophysical Research. D, Atmospheres 114 (2009) D21101, 114*. doi:10.1029/2009JD011799

Hufnagel, L., & Kocsis, M. (2011). Impacts of climate change on Lepidoptera species and communities. *Applied Ecology and Environmental Research, 9*(1), 43-72.

Iltis, C. (2019). *Impacts of climate change on the performance of an insect pest and associated consequences for tritrophic interactions.* Université Bourgogne Franche-Comté. Retrieved from https://tel.archives-ouvertes.fr/tel-02479851 Star| Univ-bourgogne| Agreenium| Cnrs database. (2019UBFCK051)

Iltis, C., Moreau, J., Pecharová, K., Thiéry, D., & Louâpre, P. (2020). Reproductive performance of the European grapevine moth Lobesia botrana (Tortricidae) is adversely affected by warming scenario. *Journal of Pest Science, 93*(2), 679-689. doi:10.1007/s10340-020-01201-1

Ioriatti, C., Anfora, G., Tasin, M., De Cristofaro, A., Witzgall, P., & Lucchi, A. (2011). Chemical Ecology and Management of Lobesia botrana (Lepidoptera: Tortricidae). *Journal of Economic Entomology, 104*(4), 1125-1137. doi:10.1603/ec10443

IPCC. (2018). *In: Global Warming of 1.5°C. An IPCC Special Report on the impacts of global warming of 1.5°C above pre-industrial levels and related global greenhouse gas emission pathways, in the context of strengthening the global response to the threat of*

climate change, sustainable development, and efforts to eradicate poverty. Geneva, Switzerland.

Jacob, D., Petersen, J., Eggert, B., Alias, A., Christensen, O. B., Bouwer, L. M., . . . Yiou, P. (2014). EURO-CORDEX: new high-resolution climate change projections for European impact research. *Regional Environmental Change, 14*(2), 563-578. doi:10.1007/s10113-013-0499-2

Jones, G. (2007). Climate change: observations, projections, and general implications for viticulture and wine production. *Economics Department-working paper, 7*, 14.

Jones, G. (2013). *Uma Avaliação do Clima para a Região Demarcada do Douro: Uma análise das condições climáticas do passado, presente e futuro para a produção de vinho.* (ADVID - Associação para o Desenvolvimento da Viticultura Duriense ed.).

Kearney, M. R., Briscoe, N. J., Karoly, D. J., Porter, W. P., Norgate, M., & Sunnucks, P. (2010). Early emergence in a butterfly causally linked to anthropogenic warming. *Biology Letters, 6*(5), 674-677.

Kendall, M. G. (1975). *Rank correlation methods*. London: Griffin.

Koenigk, T., Brodeau, L., Graversen, R. G., Karlsson, J., Svensson, G., Tjernström, M., . . . Wyser, K. (2013). Arctic climate change in 21st century CMIP5 simulations with EC-Earth. *Climate Dynamics, 40*(11), 2719-2743. doi:10.1007/s00382-012-1505-y

Kyselý, J., & Plavcová, E. (2010). A critical remark on the applicability of E-OBS European gridded temperature data set for validating control climate simulations. *Journal of Geophysical Research, 115*. doi:10.1029/2010JD014123

Lucas-Picher, P., Somot, S., Déqué, M., Decharme, B., & Alias, A. (2013). Evaluation of the regional climate model ALADIN to simulate the climate over North America in the CORDEX framework. *Climate Dynamics, 41*(5), 1117-1137. doi:10.1007/s00382-012-1613-8

Mann, H. B. (1945). Nonparametric Tests Against Trend. *Econometrica, 13*(3), 245-259. doi:10.2307/1907187

Martín-Vertedor, D., Ferrero-García, J., & Torres-Vila, L. M. (2010). Global warming affects phenology and voltinism of Lobesia botrana in Spain. *Agricultural and Forest Entomology, 12*, 169-176. doi:10.1111/j.1461-9563.2009.00465.x

Menut, L., Tripathi, O. P., Colette, A., Vautard, R., Flaounas, E., & Bessagnet, B. (2013). Evaluation of regional climate simulations for air quality modelling purposes. *Climate Dynamics, 40*(9), 2515-2533. doi:10.1007/s00382-012-1345-9

Miao, C., Su, L., Sun, Q., & Duan, Q. (2016). A nonstationary bias-correction technique to remove bias in GCM simulations. *Journal of Geophysical Research: Atmospheres, 121*(10), 5718-5735. https://doi.org/10.1002/2015JD024159

Milonas, P. G., Savopoulou□Soultani, M., & Stavridis, D. G. (2001). Day□degree models for predicting the generation time and flight activity of local populations of Lobesia botrana (Den. & Schiff.)(Lep., Tortricidae) in Greece. *Journal of Applied Entomology, 125*(9□10), 515-518.

Moreira, J. G. V., & Naghettini, M. (2016). Detecção de Tendências Monotônicas Temporais e Relação com Erros dos Tipos I e II: Estudo de Caso em Séries de Precipitações Diárias Máximas Anuais do Estado do Acre. *Revista Brasileira de Meteorologia, 31*, 394-402.

Nagarkatti, S., Tobin, P. C., & Saunders, M. C. (2001). Diapause Induction in the Grape Berry Moth (Lepidoptera: Tortricidae). *Environmental Entomology - ENVIRON ENTOMOL, 30*, 540-544. doi:10.1603/0046-225X-30.3.540

Ortega-Lopez, V., Amo-Salas, M., Ortiz-Barredo, A., & Diez-Navajas, A. M. (2014). Male flight phenology of the European grapevine moth Lobesia botrana (Lepidoptera: Tortricidae) in different wine-growing regions in Spain. *Bull Entomol Res, 104*, 566-575.

Ramos, M. C. (2017). Projection of phenology response to climate change in rainfed vineyards in north-east Spain. *Agricultural and Forest Meteorology, 247*, 104-115.

Reineke, A., & Thiéry, D. (2016). Grapevine insect pests and their natural enemies in the age of global warming. *Journal of Pest Science, 89*(2), 313-328.

Reis, S., Fraga, H., Carlos, C., Silvestre, J., Eiras-Dias, J., Rodrigues, P., & Santos, J. A. (2020). Grapevine Phenology in Four Portuguese Wine Regions: Modeling and Predictions. *Applied Sciences, 10*(11), 3708.

Riedl, H., Croft, B. A., & Howitt, A. J. (1976). Forecasting codling moth phenology based on pheromone trap catches and physiological-time models. *The Canadian Entomologist, 108*(5), 449-460.

Rockel, B., Will, A., & Hense, A. (2008). The regional climate model COSMO-CLM (CCLM). *Meteorologische Zeitschrift - METEOROL Z, 17*, 347-348. doi:10.1127/0941-2948/2008/0309

Santos, M., Fonseca, A., Fraga, H., Jones, G., & Santos, J. A. (2020). Bioclimatic conditions of the Portuguese wine denominations of origin under changing climates. *International Journal of Climatology, 40*(2), 927-941. https://doi.org/10.1002/joc.6248

Sen, P. K. (1968). Estimates of the Regression Coefficient Based on Kendall's Tau. *Journal of the American Statistical Association, 63*(324), 1379-1389. doi:10.2307/2285891

Spinoni, J., Barbosa, P., Bucchignani, E., Cassano, J., Cavazos, T., Christensen, J. H., . . . Dosio, A. (2020). Future Global Meteorological Drought Hot Spots: A Study Based on CORDEX Data. *Journal of Climate, 33*(9), 3635-3661. doi:10.1175/jcli-d-19-0084.1

Stefanescu, C., Peñuelas, J., & Filella, I. (2003). Effects of climatic change on the phenology of butterflies in

the northwest Mediterranean Basin. *Global Change Biology, 9*(10), 1494-1506.

Taylor, R. A. J., Herms, D. A., Cardina, J., & Moore, R. H. (2018). Climate change and pest management: Unanticipated consequences of trophic dislocation. *Agronomy, 8*(1), 7.

Thiéry, D., Louâpre, P., Muneret, L., Rusch, A., Sentenac, G., Vogelweith, F., . . . Moreau, J. (2018). Biological protection against grape berry moths. A review. *Agronomy for Sustainable Development, 38*(2), 15. doi:10.1007/s13593-018-0493-7

Tobin, P. C., Nagarkatti, S., Loeb, G., & Saunders, M. C. (2008). Historical and projected interactions between climate change and insect voltinism in a multivoltine species. *Global Change Biology, 14*(5), 951-957. https://doi.org/10.1111/j.1365-2486.2008.01561.x

Tobin, P. C., Nagarkatti, S., & Saunders, M. C. (2001). Modeling Development in Grape Berry Moth (Lepidoptera: Tortricidae). *Environmental Entomology, 30*(4), 692-699, 698.

Tobin, P. C., Nagarkatti, S., & Saunders, M. C. (2002). Diapause Maintenance and Termination in Grape Berry Moth (Lepidoptera: Tortricidae). *Environmental Entomology, 31*(4), 708-713. doi:10.1603/0046-225x-31.4.708

Tramblay, Y., Ruelland, D., Somot, S., Bouaicha, R., & Servat, E. (2013). High-resolution Med-CORDEX regional climate model simulations for hydrological impact studies: a first evaluation of the ALADIN-Climate model in Morocco. *Hydrol. Earth Syst. Sci., 17*(10), 3721-3739. doi:10.5194/hess-17-3721-2013

Ünlü, L., Akdemir, B., Ögür, E., & Şahin, İ. (2019). Remote Monitoring of European Grapevine Moth, Lobesia botrana (Lepidoptera: Tortricidae) Population Using Camera-Based Pheromone Traps in Vineyards. *Turkish Journal of Agriculture - Food Science and Technology, 7*, 652. doi:10.24925/turjaf.v7i4.652-657.2382

Voldoire, A., Sanchez-Gomez, E., Salas y Mélia, D., Decharme, B., Cassou, C., Sénési, S., . . . Chauvin, F. (2013). The CNRM-CM5.1 global climate model: description and basic evaluation. *Climate Dynamics, 40*(9), 2091-2121. doi:10.1007/s00382-011-1259-y

Woiwod, I. (1997). Detecting the effects of climate change on Lepidoptera. *Journal of Insect Conservation, 1*(3), 149-158.

Yenigun, K., Gumus, V., & Bulut, H. (2008). Trends in streamflow of the Euphrates basin, Turkey. *Proceedings of The Institution of Civil Engineers-water Management - PROC INST CIVIL ENG-WATER MAN, 161*, 189-198. doi:10.1680/wama.2008.161.4.189.